Air-Stable Gold Nanoparticles Ligated by Secondary Phosphine Oxides as Catalyst for the Chemoselective Hydrogenation of Substituted Aldehydes: a Remarkable Ligand Effect

Israel Cano,[†] Miguel A. Huertos,[†] Andrew M. Chapman,[†] Gerd Buntkowsky,[§] Torsten Gutmann,[§] Pedro B. Groszewicz,[§] and Piet W. N. M. van Leeuwen*[†,‡]

[†]Institute of Chemical Research of Catalonia (ICIQ), 43007 Tarragona, Spain

[§]Eduard-Zintl Institut for Inorganic and Physical Chemistry, 64287 Darmstadt, Germany

[‡]Laboratoire de Physique et Chimie des Nano Objets, LPCNO, UMR5215 INSA-UPS-CNRS, Institut National des Sciences Appliquées, Université de Toulouse, 135 avenue de Rangueil, 31077 Toulouse, France

S *Supporting Information*

ABSTRACT: Air-stable and homogeneous gold nanoparticles (AuNPs, **1a−5a**) ligated by various secondary phosphine oxides (SPOs), $[R^1R^2P(O)H]$ (R^1 = Naph, R^2 = ^tBu, **L1**; R^1 = R^2 = Ph, **L2**; R^1 = Ph, R^2 = Naph, **L3**; R^1 = R^2 = Et, **L4**; R^1 = R^2 = Cy, **L5**; R^1 = R^2 = ^tBu, **L6**), with different electronic and steric properties were synthesized via $NaBH_4$ reduction of the corresponding Au(I)−SPO complex. These easily accessible ligands allow the formation of well dispersed and small nanoparticles (size 1.2−2.2 nm), which were characterized by

the use of a wide variety of techniques, such as transmission electron microscopy, thermogravimetric analysis, UV−vis, energy-dispersive X-ray, X-ray photoelectron spectroscopy (XPS), attenuated total reflectance Fourier transform infrared spectroscopy (ATR FT-IR), and cross polarization magic angle spinning (CP MAS) NMR spectroscopy. A pronounced ligand effect was found, and CP MAS NMR experiments enabled us to probe important differences in the polarity of the P−O bond of the SPOs coordinated to the nanoparticle surface depending on the type of substituents in the ligand. AuNPs containing aryl SPOs carry only SPO anions and are highly selective for aldehyde hydrogenation. AuNPs of similar size made with alkyl SPOs contain also SPOH, hydrogen bonded to SPO anions. As a consequence they contain less Au(I) and more Au(0), as is also evidenced by XPS. They are less selective and active in aldehyde hydrogenation and now show the typical activity of Au(0)NPs in nitro group hydrogenation.
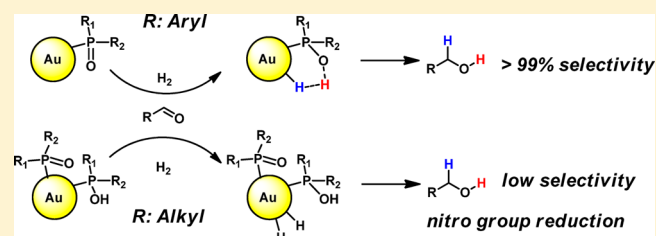
INTRODUCTION

The synthesis and characterization of gold nanoparticles (AuNPs) is an area of continuous research and has attracted much interest. A large number of studies have been reported in this field in the past decade. The formation of AuNPs has been described with thiols,[1,2] polymers,[1a,c,d] carbenes,[3] amines,[1a,d,4] thioethers,[1a] alkynes,[5] phosphines,[1,6] amino acids,[1b] etc. Especially AuNPs surrounded by thiolates have been extensively investigated. They can be synthesized in a controlled manner to give sizes that vary from small clusters with a high thiolate/Au ratio up to AuNPs with diameters of 10 nm or more. Several atomically precise nanoclusters have been reported including their X-ray structures. It occurred to us that RR′PO anions (SPO, secondary phosphine oxide) might be interesting alternatives, because their properties can be easily varied, electronically and sterically. They are much bulkier than most thiolates used, but their P-donor atom will have ligand properties similar to the S atom in thiolates.

SPOs are strong donor ligands,[7,8] relatively easy to synthesize, and more air-stable than phosphines. They are an important class of compounds that exist as an equilibrium of

the pentavalent phosphine oxide and the trivalent phosphinous acid. This equilibrium favors for most R-groups the air-stable pentavalent state but is driven toward the phosphinite tautomeric form in the presence of a coordinating metal (Scheme 1a).[9] As shown, the ligand may coordinate as the neutral acid, the deprotonated phosphinito anion, or a hydrogen bonded pair of the two, for which SPOs have a strong preference in metal complexes thus obtaining a monoanionic bidentate ligand. The phosphinito complexes so formed have an ability to cleave H_2 heterolytically across M and O, provided that there is a vacancy on the metal (Scheme 1b), and subsequently, the complex can transfer the hydrogen atoms to a suitably polarized substrate.[10]

While the formation of SPO−metal complexes[7,8,10,11] and their subsequent application in homogeneous catalysis have been extensively explored,[8,10,12] the use of secondary phosphine oxides as supporting ligands to synthesize and stabilize metal nanoparticles (MNPs) is still in its infancy. In two previous

Scheme 1. (a) Tautomeric Forms of SPOs and Formation of Metal Complexes and (b) Heterolytic Cleavage of H₂
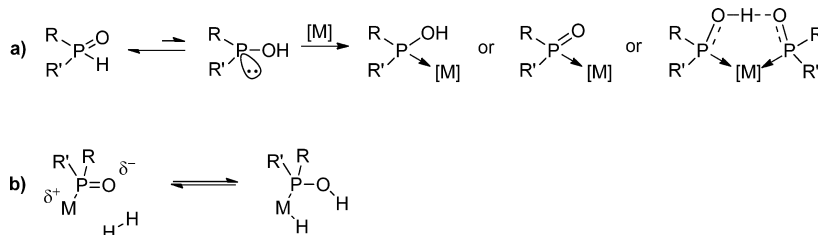
communications, we proposed that SPOs coordinated to MNPs might also act as heterolytic activators for dihydrogen together with a neighboring metal atom (Scheme 2a).[13] It was thought

Scheme 2. (a) Proposed Heterolytic Cleavage of Hydrogen on MNPs and (b) Hydrogenation of Aldehydes
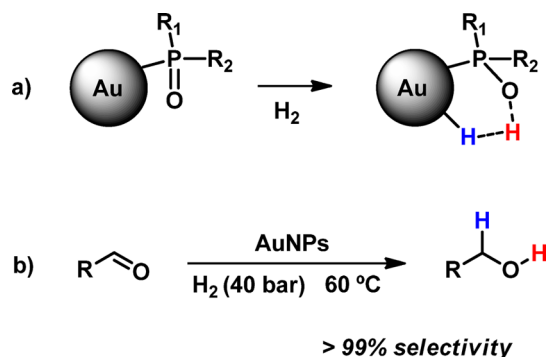
that this heterolytic pair of hydrogens would prefer the hydrogenation of C=O bonds over that of alkenes or aromatics. Along this line, our group investigated the formation of RuNPs stabilized with SPO ligands and their application in the catalytic hydrogenation of aromatic substrates; indeed, we observed a shift in selectivity from hydrogenation of aromatics to ketones when comparing a monophosphine and an SPO, but the effect was small (the selectivity for 1-phenylethanol increases from 26% to 47%).[14] In a second communication, we recently reported the synthesis of air-stable gold nanoparticles coated with *tert*-butyl(naphthalen-1-yl)phosphine oxide L1 by chemical reduction of a Au(I)−SPO precursor, 1.[15] These AuNPs were active catalysts for the highly chemoselective hydrogenation of substituted aldehydes (Scheme 2b), providing high conversions and complete selectivities for a wide range of aldehydes, not reducing a wide range of functional groups, including nitro groups and the alkenes of α,β-unsaturated aldehydes. A series of control experiments showed that the SPO ligand is a prerequisite for this catalytic activity, thus asserting a heterolytic hydrogenation mechanism. Spectroscopic studies proved that the SPO coordinates as a densely packed layer to the AuNP surface in its anionic form, Au−P(O)R₂, indeed resembling the thiolate

AuNPs. One might wonder how such a densely packed surface can still be an active catalyst, but we assume that the surface only has to accommodate a hydride and that the transfer to aldehyde is an outer-sphere process.

Multinuclear solid state NMR techniques have been used to characterize the structure of ligands on metal nanoparticles and their surface chemistry as summarized in some recent reviews.[16] Particularly, ³¹P solid state NMR has been utilized to identify the coordination and exchange dynamics of phosphine ligands,[17] as well as surface ligands derived from primary phosphine ligands on AuNPs.[18] ¹³C solid state NMR was applied to determine coordination properties of N-heterocyclic carbenes,[19] the self-assembly of polyelectrolytes and amyloid derived peptides,[20] and gold nanoparticle-doped silk films.[21]

In this study, we use a series of secondary phosphine oxide ligands for the synthesis of gold nanoparticles in order to investigate the ligand effect on their morphology and catalytic properties. To this end, a group of strongly donating SPOs differing in the steric and electronic properties was chosen for the formation of the corresponding AuNPs (Figure 1). Indeed, a very profound ligand effect has been observed.

First, the synthesis and characterization of Au(I) precursor complexes and SPO-stabilized Au nanoparticles will be presented in detail. Then, special attention will be paid to the investigation of the SPO ligands coordinated to the surface of Au nanoparticles by solid state NMR studies. Finally, the catalytic applications of the AuNPs toward the chemoselective and non-chemoselective hydrogenation of substituted aldehydes will be presented.

■ **RESULTS AND DISCUSSION**

Synthesis and Characterization of SPO-Stabilized Au Nanoparticles. Since small AuNPs of thiolates can nowadays be prepared with high selectivity in several instances,[2,22] it was thought that a general method for the study of a ligand effect would be the exchange of thiolates by SPO ligands with the intention of leaving the AuNP cores intact, which can be effectively achieved for thiolate−thiolate exchange, as published for Au[23] and, recently, for Ag.[24] To our surprise, no exchange was found so far, and instead we established that thermodynamics drove the reaction in the opposite direction! Therefore, we chose the same protocol that was used for the preparation of
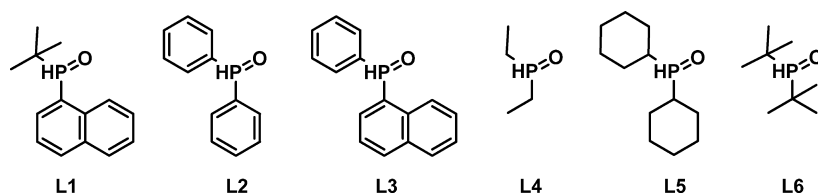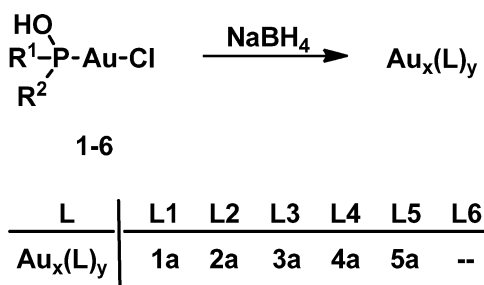

Figure 1. Secondary phosphine oxides employed in this study.

AuNPs ligated by (^{t}Bu)(Naph)P(O)H (AuNPs@^{t}Bu,Naph, **1a**), a method that may give NPs of different sizes.[15] The selected gold complexes, **2**–**5** (Scheme 3, for further details see

Scheme 3. Formation of AuNPs from Au(I)–SPO Complexes 1–5[a]

$$\begin{array}{c} \text{HO} \\ | \\ \text{R}^1\text{–P–Au-Cl} \\ | \\ \text{R}^2 \end{array} \quad \xrightarrow{\text{NaBH}_4} \quad \text{Au}_x(\text{L})_y$$

1-6

L	L1	L2	L3	L4	L5	L6
Au$_x$(L)$_y$	1a	2a	3a	4a	5a	--

[a]Reagents and conditions: 16 equiv of NaBH$_4$, THF/H$_2$O (1.4:1), 0 → 25 °C, 15 h.

section 3, Supporting Information), in cooled THF were treated with a freshly prepared solution of NaBH$_4$ in water, leading to a change in color from colorless to deep red-brown and vigorous gas evolution. After stirring overnight, the resulting AuNPs (**2a**–**5a**) were purified by a procedure similar to that used for **1a** (Scheme 3, for more details see the Supporting Information).[15] In contrast, it was not possible to generate NPs from **6** (Scheme 3) and Au(0) precipitated, due to loss of phosphine oxide probably related to the steric bulk of two ^{t}Bu groups.[25]

The purified AuNPs were characterized by several techniques. Transmission electron microscopy (TEM) analysis revealed the presence of well dispersed and small nanoparticles (Figure 2, for more details see the Supporting Information) with an average size in the range 1.2–2.2 nm [**1a**, 1.24(0.16) nm;[15] **2a**, 1.61(0.16) nm; **3a**, 2.02(0.17) nm; **4a**, 2.20(0.19) nm; **5a**, 1.58(0.13) nm]. UV–vis spectra of **1a**–**5a** (section 6, Supporting Information) show the absence of a plasmon resonance band, as is to be expected for nanoparticles of this size.[1b,26]

Note that the histograms are based on number-averaged diameters as is commonly done in this field, while for the composition a weight-averaged presentation is more realistic; the weight increases with the cube of the diameter and thus even in these narrow distributions one should not neglect this when considering the composition.[27] In a discussion of catalytic properties, for example, a size effect on rate, one might rather use a surface averaged histogram!

Elemental analysis (EA), thermogravimetric analysis (TGA), and energy-dispersive X-ray analysis (EDX) were performed with the aim of elucidating the percentage of metal contained in the nanoparticles. The Au content was in the range of 44–50% for **1a**–**3a** and 63–66% for **4a** and **5a**, while EA and EDX displayed the absence of chloride in the nanoparticles (section 5, Supporting Information). EA, TGA, and EDX (see the Supporting Information) are consistent with a metal–ligand ratio of 1.48:1 for **1a**, 1.32:1 for **2a**, 1.63:1 for **3a**, 1.84:1 for **4a**, and 2.88:1 for **5a** (Table 1). It is worth noting that in the case of SPOs with aromatic substituents (**1a**–**3a**), the Au/L ratio accounts for a large amount of phosphine coordinated to the surface of the nanoparticle. On the other hand, AuNPs formed
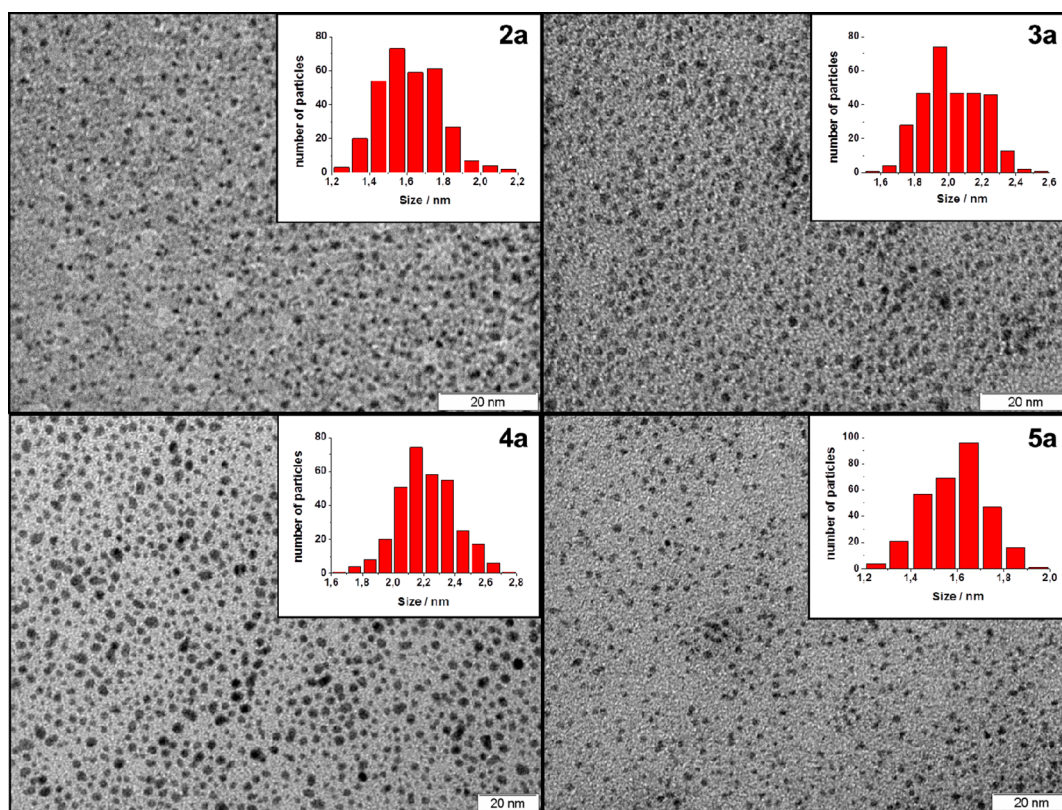

Figure 2. Representative TEM images of AuNPs **2a**–**5a** and size distributions determined from TEM images by counting >300 nontouching particles obtained from images captured from distinct quadrants of the grid.

Table 1. Analytical Data of the AuNPs

AuNP	size (nm)	Au content (%)[a]	Au/L ratio	Au_x/L_y[b]	N_s[c]
1a	1.24 ± 0.16	46.8	1.48:1	50/35	40
2a	1.61 ± 0.16	49.6	1.32:1	120/90	90
3a	2.02 ± 0.17	44.5	1.63:1	230/140	130
4a	2.20 ± 0.19	62.9	1.84:1	290/160	160
5a	1.58 ± 0.13	66.1	2.88:1	110/40	80
6a	∞	100	∞	∞	∞

[a]Average[28] of EA, TGA, and EDX analysis. [b]The approximate composition is based on the Au/L ratio and the number-average size measured. [c]Number of surface atoms. Approximate values obtained from the graphs of Van Hardeveld and Hartog.[29]

with completely aliphatic SPOs (**4a** and **5a**) showed higher Au contents and Au/L ratios. The differences in ligand content are attributed to the steric and electron-donor properties of these aliphatic SPOs. The sizes and Au/L ratios do not necessarily reflect the thermodynamic stability of the AuNPs formed, but rather they are the result of the metal particle growth rate and the rate of ligand dissociation or complexation during their synthesis. In the case of SPOs, the rate and extent by which the anions are formed may also influence the nanoparticle growth. Larger particles contain a smaller fraction of surface atoms and on flatter surfaces there is more steric hindrance of the ligands. Within the group of alkyl ligands, there is consistency of the influence of the size, but the smallest aliphatic ligand, **L4**, is much smaller than the preceding aromatic ligands. Ligands **L5** and **L1** have similar sizes, but the particles formed are much larger for **L5**. The most bulky and electron rich **L6** gives Au metal. Thus, the electronic properties may play a role here. We observed a decrease of stability of the corresponding Au(I)–SPOH complexes, as noticed from the precipitation of Au(0), following an increase in the electron-donor character of the substituents, Cy and ^{t}Bu. Therefore, the loss of ligand in the process of formation of the AuNPs might be faster. Consequently, the surface of the nanoparticle contains less ligand and the metal–ligand ratio is higher for Cy_2POH, **L5**, and even zero ligands for $^tBu_2POH$, **L6**.

Table 1 shows that, except **5a**, which contains the most bulky dicyclohexyl ligand, the approximate number of surface atoms is close to the number of SPO ligands, as is also the case for thiolates and Au surface atoms in Au nanoclusters based on thiolates. All values are rounded-off, approximate values because a high accuracy cannot be obtained.

Attenuated total reflectance Fourier transform infrared (ATR FT-IR) spectra exhibit clear differences between **1a–3a** on the one hand and **4a** and **5a** on the other hand (section 7, Supporting Information). While **1a–3a** spectra display no O–H stretching absorption, in the spectra of **4a** and **5a** a broad band of moderate intensity between 3000 and 3500 cm^{-1} is observed (Figures S19 and S22, Supporting Information). Both the differences detected in the metal–ligand ratio and the presence of a possible O–H stretching vibration in the case of **4a** and **5a** can be ascribed to the different electronic properties of alkyl- and aryl-substituted SPOs, that is, the higher basicity of alkyl SPOs. We recently demonstrated the presence of O–H in Ru nanoparticles stabilized by SPO ligands by H_2/D_2 isotope exchange reaction.[14] In order to identify this band as the expected P–O–H stretching absorption, we prepared the ^{2}H-labeled nanoparticles **5a-D** from the corresponding SPO-D (**L5-^{2}H**) with the aim to observe an isotopic shift. Indeed, the O–H band had disappeared in the spectrum of **5a-D**, but the

corresponding P–O–D stretching absorption was not detected (Figure S25, Supporting Information). Finally, the ATR FT-IR spectrum of free **L** shows the P–H stretching absorption in the range of 2280–2360 cm^{-1}, while this band was not found in the ATR FT-IR spectra of the corresponding AuNPs (section 7, Supporting Information), proving that the ligand in nanoparticles **1a–3a** is bound as Au–P(O)R$_2$.[15] We have attempted to identify the intermediate H_2 adducts of these catalysts under H_2 pressure by IR, but the addition product(s) AuH and R$_2$POH were not observed up to 40 bar.

The presence of the protons in **4** and **5** and the lower ligand coverage in **5** lead to a different total charge of the Au cores of the two types of AuNPs. This difference is observable in the Au 4f X-ray photoelectron (XPS) spectra of **1a**, **2a**, and **5a** (Figure 3 and section 8, Supporting Information). Previously X-ray
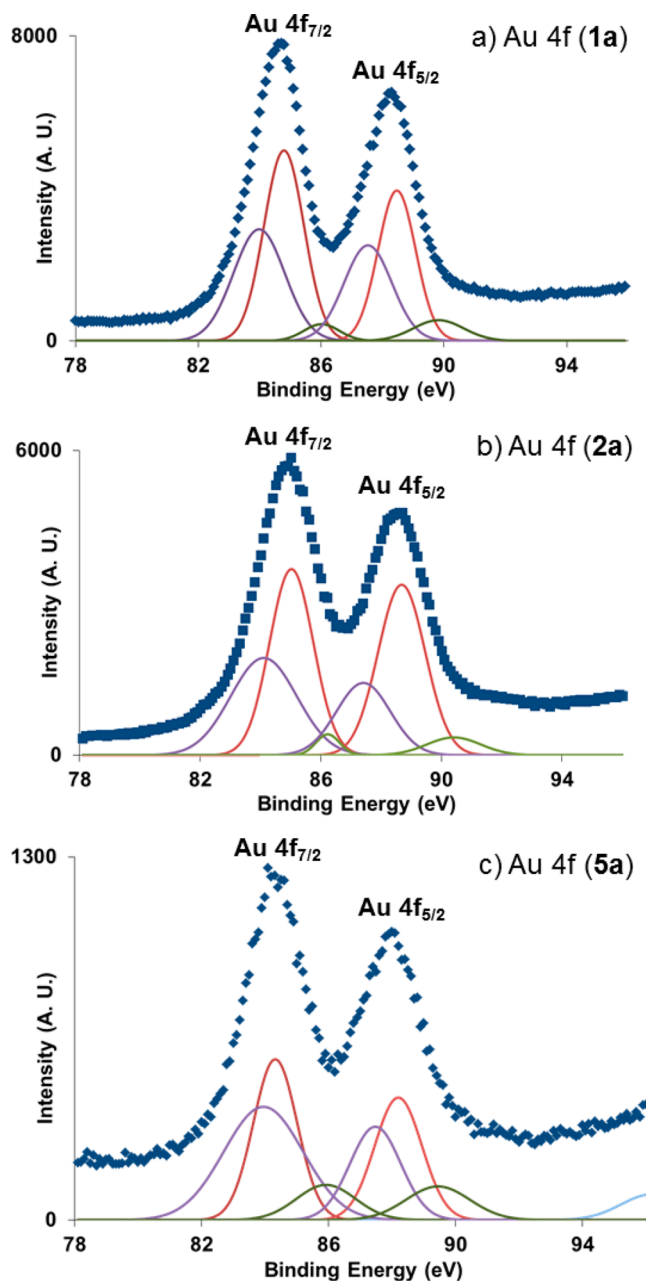
Figure 3. XPS spectra of Au 4f with fitting for (a) **1a**, (b) **2a**, and (c) **5a**.

spectroscopy has been successfully used to study the valence state of Au nanoclusters and NPs.[30] For instance, XPS spectra taken during the adsorption of Au(III) ions over thiol-capped magnetite nanoparticles, Fe_2O_3@DMSA (DMSA = dimercap-tosuccinic acid), allowed the authors to monitor the various oxidation states of gold in the process.[31] In the present study, **1a** and **2a** exhibit a binding energy for Au $4f_{7/2}$ of 84.8 and 84.9 eV, respectively, showing a decrease in energy compared with Au(I) species (85.5−86 eV)[31,32] but a higher value than that found for Au(0) (83.8 eV is regarded as metallic Au).[31,33] This behavior can be expected since nanoparticles **1a−5a** consist of a mixture of Au(0) and Au(I). As NPs, **1a** are smaller than **2a** and the number of surface gold atoms (Au(I)) is higher. However, the electronic donation of the *tert*-butyl substituent in **1a** neutralizes this effect and produces a displacement in the energy toward the bulk metal values, indeed showing a binding energy lower than **2a**. On the other hand, a negative shift in the Au (4f) binding energy was observed for **5a** (84.4 eV) in comparison to those of **1a** and **2a** (0.5 ± 0.05 eV relative to **2a**). The XPS spectra were fitted with three contributions (Figure 3). For **5a**, the area of the metallic Au absorption increases in comparison to those of **1a** and **2a**. Not only does the surface of **5a** contain fewer ligands, but also in part they are neutral ligands, R_2P-O-H, and therefore **5a** contains relatively more Au(0) than NPs **1a−3a**.

Solid State NMR Studies. *General.* Although solution NMR is a proper tool for the investigation of the SPO ligands, it could not deliver conclusive insights for AuNPs **1a−5a**, probably due to slow molecular tumbling, Knight-shift-induced line broadening, exchange-induced line-shape effects, etc.[34] Hence, magic angle spinning solid-state NMR (MAS NMR) was performed to characterize the SPO ligands coordinated to the surface of the Au nanoparticles. An extensive study was made by comparison of the ^{31}P and ^{13}C NMR spectra of AuNPs and free ligands for various SPO ligand systems, which constitutes the basis for understanding the different catalytic properties of these nanoparticles.

[31]P Cross-Polarization (CP) MAS NMR. The ^{31}P chemical shift is directly connected to the electron distribution around this nucleus. Therefore, the chemical shift might be able to express properties such as the polarity of the P=O bond as a function of ^{31}P deshielding when different substituents and ligand states are compared (i.e., free ligand, AuNP). Figure 4 displays the ^{31}P NMR CP MAS spectra of the SPO stabilized AuNPs **1a−5a**, and Table 2 collects the relevant NMR parameters extracted from the spectra.

The main results of this analysis are described in the following. By comparing the δ_{iso} values for each SPO as a free ligand and in the AuNP, a clear trend toward higher values (more deshielded nuclei) is observed when the ligand coordinates to the AuNPs. This change is described as the complexation shift[36] ($\Delta\delta$), the values of which are also summarized in Table 2. Due to the ligand-to-metal electronic donation, the interaction of SPOs with gold particles leads to a deshielding of the ^{31}P nuclei, and possibly to a more polarized P=O bond. While for the aromatic compounds **1a**, **2a**, and **3a**, a complexation shift ($\Delta\delta$) in the range between 85 and 100 ppm is observed, for the aliphatic compounds **4a** and **5a** values of ca. 76 ppm are found. This difference strongly suggests a higher polarity of the P−O bond for the aromatic SPOs than for aliphatic ones.

The isotropic chemical shift value, δ_{iso}, is the mean value corresponding to the electronic distribution around the
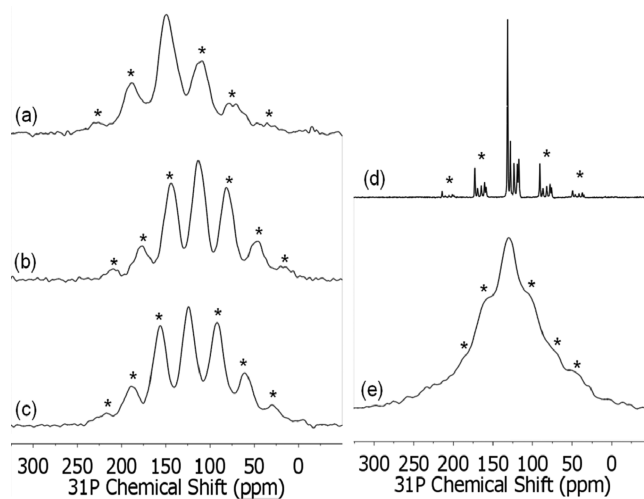

Figure 4. [31]P CP MAS spectra of AuNPs (a) **1a**, (b) **2a**, and (c) **3a** measured at 9.4 T corresponding to a frequency of 162.00 MHz, as well as (d) **4a** and (e) **5a** measured at 14.1 T corresponding to a frequency of 242.94 MHz. Asterisks mark spinning sidebands. MAS frequencies of 5 (a−c), 10 (d), and 7 kHz (e) were employed.

phosphorus nuclei in SPOs. However, it lacks information on the spatial orientation of the electronic distribution around this nucleus. This information can be revealed by solid-state NMR in the form of the chemical shift anisotropy, δ_{CSA}, which describes the orientation dependence of the electronic shielding via the CSA tensor. For phosphine oxides, the most shielded component, δ_{33}, of the chemical shift tensor usually lies along the P=O bond,[37] and its difference from the isotropic chemical shift, δ_{iso}, amounts to the chemical shift anisotropy, δ_{CSA}. Table 2 shows that a value of 80 ppm for δ_{CSA} is consistently observed for the AuNPs stabilized with aryl-substituted ligands **1a−3a**. This value decreases to around 60 ppm for **4a** and **5a**, which are stabilized by aliphatic ligands. Larger δ_{CSA} values stand for larger differences in electron density along the P−O axis and the perpendicular orientations. Hence, the larger δ_{CSA} values observed for **1a−3a** indicate a much stronger P−O bond for the aromatic systems (**1a−3a**) than for the aliphatic ones (**4a** and **5a**), a fact that might influence their catalytic activity. From IR, we know that the aromatic SPO−NPs contain SPO anions and thus indeed a P=O double bond. In contrast, the aliphatic ones contain at least in part the neutral ligands, R_2P-O-H, or they exist as H-bonded dimers as we often found in homogeneous complexes $R_2P-O-H\cdots O=PR_2$. The bond order for these P−O bonds is reduced compared with the aromatic ones. Therefore, the aliphatic ligands present a longer and consequently less polarized bond between P and O, which is also reflected in the CSA. As consequence of the less polarized P−O bond, the electronic density is not intensively localized along the P−O bond anymore, in contrast to the aromatic AuNPs. This more homogeneous distribution of the electronic density affords the lower values of the CSA observed for the aliphatic NPs compared with the aromatic ones. In addition to that, the local symmetry of the phosphorus nucleus in the ligand system is related to the asymmetry of the chemical shift tensor (η), which exhibited a value close to 1 for all investigated AuNPs. Such values correspond to a low symmetry around the phosphorus nuclei, which is a consequence of the large variety of atoms bonded to it (i.e., O, C, and Au).

Finally, the analysis of line width of the ^{31}P spectra (Figure 4) may provide insights on the rigidity of the ligand system

Table 2. ^{31}P NMR Parameters As a Function of Secondary Phosphine Oxide Ligands Employed^a

	^{t}Bu,Naph			diPhenyl			Ph,Naph			diEthyl			diCyclohexyl		
	L1	1a	$\Delta\delta$	L2	2a	$\Delta\delta$	L3	3a	$\Delta\delta$	L4	4a	$\Delta\delta$	L5	5a	$\Delta\delta$
δ_{iso}	56	150	94	25	112	87	26	124	98	56	132	76	53	129	76
δ_{CSA}		80			80			80			54			62	
η		0.7			1			1			1			1	

^{a}The parameters are the isotropic chemical shift, δ_{iso}, the chemical shift anisotropy, δ_{CSA}, and asymmetry parameter, η, which are deduced from the spectra by simulation with the SIMPSON software package.[35] Naph is 1-naphthyl.

coordinated to the AuNPs. While the aromatic systems **1a−3a** show similar line widths, a much broader line width is observed for the rigid cyclohexyl system **5a**. In contrast to **5a**, the diethyl system **4a** displays very narrow lines, the widths of which might be a consequence of the high mobility of the relatively small and flexible alkyl chains.

^{13}C CP MAS NMR. Figure 5 compares the ^{13}C CP NMR MAS spectra for the *tert*-butyl-naphthyl system. The spectrum

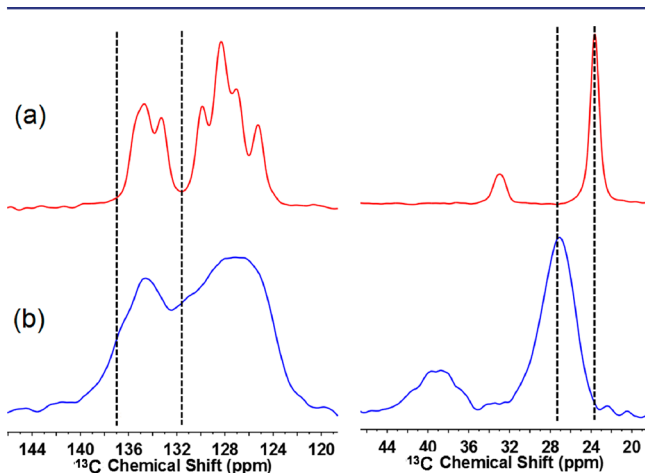**Figure 5.** ^{13}C NMR MAS spectra of the ^{t}Bu-Naph system measured at 9.4 T corresponding to a frequency of 100.59 MHz employing 6 kHz spinning: (a) free ligand **L1** and (b) AuNP **1a**. (left) Aromatic region; (right) aliphatic region. Complexation shifts signals to higher frequencies as consequence of electronic deshielding.

of the free ligand **L1** exhibits signals in two regions. The first region comprises two peaks, at 24 and 32 ppm. These correspond to the *tert*-butyl substituent (methyl moieties and tertiary carbon, respectively). Both peaks shift to higher chemical shift values in the AuNP **1a**, for which the difference amounts to 4 and 6 ppm. A similar shift is also observed for the signals from the naphthyl substituent. While the free ligand exhibits peaks around 128 and 134 ppm, for **1a** signal intensity appears at 132 and 137 ppm. This observation can be understood as a deshielding of the SPO substituent caused by the electron donation to the metal. Compared to the coordination chemical shift difference $\Delta\delta$ of about 100 ppm previously observed on ^{31}P for this system,[15] for ^{13}C this effect is smaller and relates to weak interactions of the ligand system with gold atoms. Furthermore, the comparison of the two spectra shows a broadening of the lines, which seems to be an effect of disordering of the SPO when coordinating to AuNPs, for which the formation of a complex hydrogen bonding network is expected as already shown for RuNPs.[14]
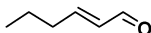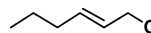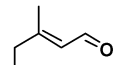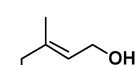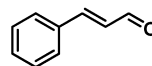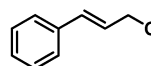
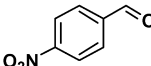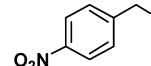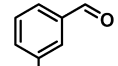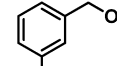**Ligand Effect in the Catalytic Hydrogenation of Aldehydes with 1a−5a.** In comparison with other metals, gold is not a typical catalyst for hydrogenation reactions, and

there are only a few reports on *homogeneous* AuNPs and most hydrogenations concern the hydrogenation of a nitro group, most often with $NaBH_4$.[2,38] This is due to the low ability exhibited by gold to dissociate hydrogen.[39] The catalytic activity of nanoparticles **1a−5a** was evaluated in the hydrogenation reaction of several substituted aldehydes (Table 3) with the purpose to find a relation between the ligand substituents and the catalytic properties. We decided to use the optimized reaction conditions that were previously described for **1a** (60 °C, 40 bar).[15] The solvent is relatively important in this type of catalysis, THF and hexane being the most favorable media to perform the experiments. Table 3 shows that there are marked differences in the catalytic behavior of nanoparticles ligated by aromatic SPOs and nanoparticles formed with completely aliphatic SPOs. AuNPs stabilized with aryl-substituted ligands (**1a−3a**) showed a high catalytic activity and a very high selectivity in the hydrogenation of aldehydes over other functional groups (>99% in all instances, Table 3).

The nanoparticles were completely selective to the carbonyl functionality in α,β-unsaturated aldehydes such as cinnamaldehyde and *trans*-2-hexen-1-al (Table 3, entries 1−3 and 11−13). Of particular interest is the selective hydrogenation of citral. This molecule is a challenging one since it contains conjugated C=O and C=C bonds and an isolated olefinic bond. The substrate was selectively hydrogenated to geraniol and nerol (*cis*- and *trans*-isomers, entries 6, 7, and 8), compounds employed in the production of perfumes and fragrances.[40] AuNPs **1a−3a** are highly tolerant of the presence of a NO_2 group. The hydrogenation of *p*-nitrobenzaldehyde provided the corresponding nitrobenzyl alcohol with excellent selectivity (entries 16, 17, and 18). Finally, complete chemoselectivity was observed in the hydrogenation of aldehydes in the presence of other carbonyl groups, such as ketones. For example, the hydrogenation of 3-acetylbenzaldehyde was performed with perfect retention of the ketone group (entries 21, 22, and 23). In nearly all cases, high conversions were obtained. We observed an increase in the activity with a decrease in the size of the NPs. The smallest ones, **1a** (1.24 nm), are the most active nanoparticles, as can be seen from the kinetic studies (Figure 6). As shown, **1a** is the most active catalyst, followed by **2a** and **3a**. This correlates with the number of surface atoms because the total amount of Au is equal for all cases. In cinnamaldehyde this is less pronounced, but the phenyl group does change the character of the enal slightly.

On the other hand, NPs ligated by aliphatic phosphine oxides (**4a** and **5a**) exhibit a different catalytic behavior; their activity is lower, while the selectivity is lost in many cases. The hydrogenation of citral and 3-acetylbenzaldehyde preserved the high selectivity observed for **1a−3a**. However, the conversions were very low (entries 9, 10, 24, and 25). A loss of selectivity was observed in the hydrogenation of *trans*-2-hexen-1-al (entries 4 and 5), obtaining the corresponding unsaturated alcohol and, additionally, an amount of the fully

Table 3. Catalytic Hydrogenation of Aldehydes with 1a–5a[a]

Entry	Substrate	AuNP	Product	Conversion (%)[b]	Selectivity (%)
1		1a		98[c]	>99[d]
2		2a		62	>99[d]
3		3a		65[c]	>99[d]
4		4a		10[c]	73[d]
5		5a		66[c]	83[d]
6		1a		79[c]	>99
7		2a		27[c]	>99
8		3a		78[c]	>99
9		4a		9	>99
10		5a		9[c]	>99
11		1a		100[c]	>99
12		2a		100	>99
13		3a		85[c]	>99
14		4a		47	>99
15		5a		48[c]	85
16		1a		100	>99
17		2a		100	>99
18		3a		94	>99
19		4a		100	20
20		5a		100	29
21		1a		96	>99
22		2a		93	>99
23		3a		80	>99
24		4a		9	>99
25		5a		3	>99

[a]Reagents and conditions: 1–5a (0.01 mmol of Au assuming % of Au from elemental analysis), substrate (entries 1–10 and 21–25, 2 mmol; entries 11–20, 4 mmol), THF (5 mL), 18 h, 60 °C, 40 bar H_2. [b]Conversions and product identities were determined by ^1H NMR spectroscopy (average of two runs). [c]Reaction was performed in hexane as solvent. [d]Reaction performed at 50 °C.
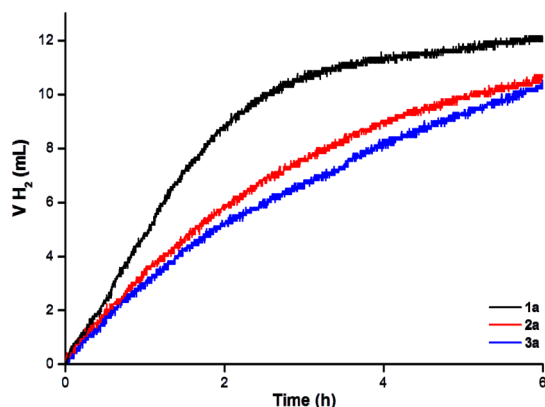

Figure 6. Graph of gas consumption for cinnamaldehyde hydrogenation. Reagents and conditions: 0.01 mmol of Au, 0.5 mmol of substrate, THF (5 mL), 60 °C, 40 bar H_2.

hydrogenated product, 1-hexanol (5% for 4a and 11% for 5a, respectively). Furthermore, 4a gave a very low conversion. The hydrogenation of cinnamaldehyde was performed with a reduced efficiency (entries 14 and 15), and in the case of 5a, a small amount of C=C hydrogenation was observed, and both 3-phenylpropanal (3%) and 3-phenylpropanol (4%) were produced as byproducts in addition to the expected product (cinnamyl alcohol, 41%). Surprisingly, the reaction catalyzed by 4a led to the unsaturated alcohol as the unique product, while the C=C bond was unaffected. Finally, it should be emphasized that the hydrogenation of 4-nitrobenzaldehyde (entries 19 and 20) provided quantitative conversions but proceeded with very low selectivity toward the nitrobenzyl alcohol (<30%), affording considerable amounts of products resulting from nitro group hydrogenation, such as 4-aminobenzaldehyde and 4-aminobenzyl alcohol (Scheme 4B,E). A noteworthy feature is the detection of azoarenes in the reaction medium (Scheme 4C). The reduction of nitroarenes to azoarenes or anilines has been described with the use of gold nanoparticles supported on metal oxides employing 2-propanol as the hydrogen donor.[41] Also, the hydrogenation of nitrobenzene to aniline can be carried out over heterogeneous AuNP/Fe_2O_3.[42] When AuNPs in solution are employed for the reduction of nitrobenzene, the common reducing agent is

Scheme 4. Hydrogenation of 4-Nitrobenzaldehyde Catalyzed by 4a and 5a[d]

AuNPs	Selectivity (% C$_6$H$_4$)				
	A	**B**	**C**[a]	**D**	**E**
4a[b]	0	10	4	**20**	52
5a[c]	0	29	19	**29**	4
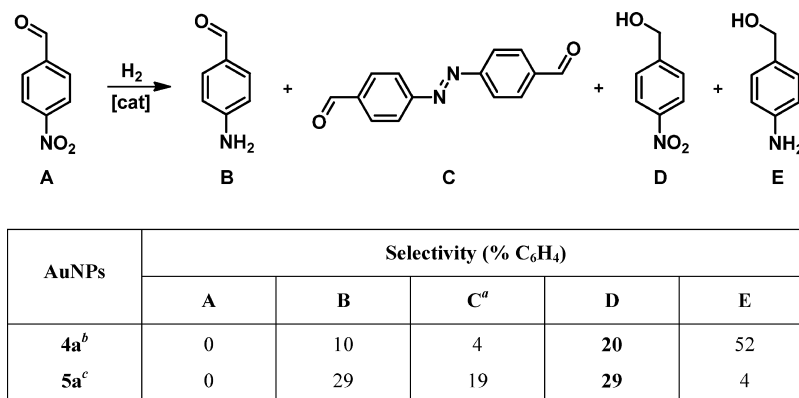
[a]Numbers from ^{1}H NMR integrals; note that C contains double the amount of aryl groups. [b]14% unidentified compound. [c]19% unidentified compound. [d]Reagents and conditions: 0.01 mmol of Au, 4 mmol of substrate, THF (5 mL), 18 h, 60 °C, 40 bar H$_2$.

NaBH$_4$.[43] In the present instance, the hydrogenation of both nitro and aldehyde groups takes place with catalysts **4a** and **5a**, which leads to the formation of a wide variety of products, reducing the selectivity.

The behavior of catalysts **1a–3a** on the one hand and catalysts **4a** and **5a** on the other hand is ascribed to a subtle change in electronic effect of the ligand system. This assumption is confirmed by the results of the solid state NMR and IR measurements. The observed trend of larger complexation shifts ($\Delta\delta$) combined with the higher chemical shift anisotropy (δ_{CSA}) values reinforces the argument that the aromatic substituents in SPOs afford R$_2$P=O anions in catalysts **1a–3a**. Since the number of surface atoms and anions is approximately the same (Table 1), all surface atoms are Au(I) species, as in many thiolate nanoclusters and nanoparticles. The more basic aliphatic R$_2$POHs **L4** and **L5** hold on more strongly to the protons and the actual ligand is R$_2$PO–H or R$_2$PO···H. According to ^{31}P NMR, the alkyl donor groups and the presence of the proton result in a less polarized P–O bond. Since R$_2$POH is a neutral ligand, the surface of **4a** and **5a** contains more, if not all, Au(0) atoms. Furthermore, **5a** has a lower ligand surface coverage (Table 1), and the metallic character increases even further. The strongest donor ligand **6** forms no AuNPs and gives an Au mirror; the steric properties perhaps also influence nanoparticle formation, but despite the vast amount of data on ligand containing MNPs, this is beyond comprehension.

Thus, Au(I)R$_2$P=O must play a role in catalysis in **1a–3a**, while molecular, saturated Au(I) species including those containing SPOH such as the precursors used here were found to be inactive.[15] We speculate that the active species is Au(SP=O) resting on a Au(0)$_n$ core, and the activity is the result of a cooperative effect between the SP=O bound to the surface and the dynamically exposed Au(0)/Au(I) surface atoms. The oxygen atom of the highly polarized SP=O functions as the Lewis base binding the proton, while Au acts as the Lewis acid capturing the hydride ion, thus giving the heterolytic cleavage of dihydrogen.

At the edges of metallic AuNPs immobilized on oxide supports, one might also expect that heterolytic cleavage can take place, although only a small number of metal atoms can participate. Au metal on oxide support was found not to be active for aldehyde hydrogenation. In this context, we should mention that the usual, accepted mechanism of activation of H$_2$ on Au with transfer of H to the support is ascribed to a spillover mechanism.[44] Corma et al. have demonstrated that Au–O–Ti is not involved in the heterolytic cleavage of H$_2$.[45] The support has a strong influence on the reactivity of AuNPs, but this may have other origins.[46] After heterolytic cleavage of H$_2$, transfer to aldehyde takes place, either via a classic insertion mechanism or via an outer sphere transfer to the carbonyl bond. The former mechanism may involve coordination of the carbonyl group to the Au Lewis acid, as was proposed for other catalysts.[2a,b] The latter is the preferred mechanism according to DFT calculations in molecular RhSPO catalysts.[10e] The highest rate coincides with the most crowded **1a**, which hints perhaps at an outer sphere mechanism. As mentioned above the hydrogen adduct could not be observed, and since the reaction rate decreases with diminishing aldehyde concentration (Figure 6), both steps occur in the rate equation and the second one is rate-limiting. The order of the two steps is not known.

Catalysts **4a** and **5a** based on aliphatic SPOs are much less active than **1a–3a**, because they contain fewer of the active sites Au(I)R$_2$P=O. The moieties AuR$_2$PO–H can function as precursors to the proposed active species, but rates will be lower. Ligand coverage is lower in **5a**, which further increases the metallic character. The metallic species present turn **4a** and **5a** into catalysts for the reduction of the nitro group, a known reaction for such species. The aniline formed reacts with the nitrosobenzene intermediate giving azobenzenes. AuNP systems have been reported that give selectively azobenzene or product mixtures as shown above. Thus, the reaction found is as to be expected for AuNPs. Interestingly, a simple change from aromatic to aliphatic SPO ligands can bring about this change.

■ CONCLUSIONS

In summary, we have successfully used a series of secondary phosphine oxide ligands for the synthesis of air-stable gold nanoparticles. Compared with most current studies in homogeneous catalysis dealing with ligand effects, we have used a small number of ligands (six), so far. In all phases, reproducible synthesis, purification, and characterization, a study of MNPs is a far more tedious task than that of homogeneous systems, although characterization is often missing in the latter as well. For both areas, there is the difficult task of establishing that one really deals with MNPs or homogeneous complexes as the catalyst![47] Therefore, we

decided to use a limited "library", so far. An extensive characterization of these AuNPs was performed by several techniques, which demonstrated that the nature of the ligand is a key feature, since important differences in the size, morphology, and catalytic behavior were found depending on the characteristics of the P-substituents. Specifically, CP-MAS NMR spectroscopy has allowed us to gain insight in the polarization of the P=O or POH bond in the different types of AuNPs. In this context, nanoparticles prepared with aryl-substituted SPOs present a strong polarity of the P=O bond and showed high catalytic activity and very high selectivity in the chemoselective hydrogenation of substituted aldehydes. On the other hand, this ability is lost in the case of NPs ligated by aliphatic phosphine oxides, which exhibit a lower polarity of the P=O bond or the presence of POH bonds instead, slowing the heterolytic cleavage of dihydrogen. The metallic nature of part of the surface atoms in the alkyl SPO AuNPs induces reduction of nitro groups, the common reaction of metallic AuNPs. In conclusion we may say that with the remarkable ligand effect reported here, SPO ligands have shown their merit in metal nanoparticle catalysis.

ASSOCIATED CONTENT

ⓈSupporting Information

Detailed experimental procedures, analytical and spectral data, and crystallographic data for **4**. The Supporting Information is available free of charge on the ACS Publications website at DOI: 10.1021/jacs.5b02802.

AUTHOR INFORMATION

Corresponding Author
*vanleeuw@insa-toulouse.fr

Notes
The authors declare no competing financial interest.

REFERENCES

(1) (a) Daniel, M.-C.; Astruc, D. *Chem. Rev.* **2004**, *104*, 293. (b) Lu, Y.; Chen, W. *Chem. Soc. Rev.* **2012**, *41*, 3594. (c) Maity, P.; Xie, S.; Yamauchi, M.; Tsukuda, T. *Nanoscale* **2012**, *4*, 4027. (d) Zhao, P.; Li, N.; Astruc, D. *Coord. Chem. Rev.* **2013**, *257*, 638. (e) See the Supporting Information for a variety of examples related to the formation of AuNPs with thiols..

(2) (a) Zhu, Y.; Qian, H.; Drake, B. A.; Jin, R. *Angew. Chem., Int. Ed.* **2010**, *49*, 1295. (b) Zhu, Y.; Qian, H.; Zhu, M.; Jin, R. *Adv. Mater.* **2010**, *22*, 1915. (c) Li, G.; Jiang, D.-e.; Kumar, S.; Chen, Y.; Jin, R.

ACS Catal. **2014**, *4*, 2463. (d) Li, G.; Zeng, C.; Jin, R. *J. Am. Chem. Soc.* **2014**, *136*, 3673. (e) Li, G.; Jin, R. *J. Am. Chem. Soc.* **2014**, *136*, 11347.

(3) (a) Vignolle, J.; Tilley, T. D. *Chem. Commun.* **2009**, *46*, 7230. (b) Rodríguez-Castillo, M.; Laurencin, D.; Tielens, F.; van der Lee, A.; Clément, S.; Guari, Y.; Richeter, S. *Dalton Trans.* **2014**, *43*, 5978.

(4) See the Supporting Information for a variety of examples related to the formation of AuNPs with amines.

(5) (a) Zhang, S.; Chandra, K. L.; Gorman, C. B. *J. Am. Chem. Soc.* **2007**, *129*, 4876. (b) Maity, P.; Tsunoyama, H.; Yamauchi, M.; Xie, S.; Tsukuda, T. *J. Am. Chem. Soc.* **2011**, *133*, 20123. (c) Maity, P.; Wakabayashi, T.; Ichikuni, N.; Tsunoyama, H.; Xie, S.; Yamauchi, M.; Tsukuda, T. *Chem. Commun.* **2012**, *48*, 6085.

(6) See the Supporting Information for a variety of examples related to the formation of AuNPs with phosphines.

(7) Martin, D.; Moraleda, D.; Achard, T.; Giordano, L.; Buono, G. *Chem.—Eur. J.* **2011**, *17*, 12729.

(8) Dubrovina, N. V.; Börner, A. *Angew. Chem., Int. Ed.* **2004**, *43*, 5883.

(9) Hoge, B.; Neufeind, S.; Hettel, S.; Wiebe, W.; Thösen, C. *J. Organomet. Chem.* **2005**, *690*, 2382.

(10) (a) van Leeuwen P. W. N. M.; Roobeek, C. F. Eur. Pat. Appl. EP 82576, 1983. *Chem. Abstr.* **1983**, *99*, 121813. (b) van Leeuwen, P. W. N. M.; Roobeek, C. F.; Wife, R. L.; Frijns, J. H. G. *J. Chem. Soc., Chem. Commun.* **1986**, 31. (c) van Leeuwen, P. W. N. M.; Roobeek, C. F.; Frijns, J. H. G.; Orpen, A. G. *Organometallics* **1990**, *9*, 1211. (d) van Leeuwen, P. W. N. M.; Roobeek, C. F. *New J. Chem.* **1990**, *14*, 487. (e) Castro, P. M.; Gulyas, H.; Benet-Buchholz, J.; Bo, C.; Freixa, Z.; van Leeuwen, P. W. N. M. *Catal. Sci. Technol.* **2011**, *1*, 401.

(11) (a) Chatt, J.; Heaton, B. T. *J. Chem. Soc. A* **1968**, 2745. (b) Dixon, K. R.; Rattray, A. D. *Can. J. Chem.* **1971**, *49*, 3997. (c) Kraihanzel, C. S.; Bartish, C. M. *J. Am. Chem. Soc.* **1972**, *94*, 3572. (d) Beaulieu, W. B.; Rauchfuss, T. B.; Roundhill, D. M. *Inorg. Chem.* **1975**, *14*, 1732. (e) Lindner, E.; Schilling, B. *Chem. Ber.* **1977**, *110*, 3266. (f) Hollatz, C.; Schier, A.; Schmidbaur, H. *J. Am. Chem. Soc.* **1997**, *119*, 8115. (g) Hollatz, C.; Schier, A.; Schmidbaur, H. *Inorg. Chem. Commun.* **1998**, *1*, 115. (h) Hollatz, C.; Schier, A.; Riede, J.; Schmidbaur, H. *J. Chem. Soc., Dalton Trans.* **1999**, 111. (i) Hollatz, C.; Schier, A.; Schmidbaur, H. *Inorg. Chim. Acta* **2000**, *300–302*, 191. (j) Zhou, Y.; Yin, S.; Gao, Y.; Zhao, Y.; Goto, M.; Han, L.-B. *Angew. Chem., Int. Ed.* **2010**, *49*, 6852. (k) Christiansen, A.; Selent, D.; Spannenberg, A.; Baumann, W.; Franke, R.; Börner, A. *Organometallics* **2010**, *29*, 3139.

(12) (a) Li, G. Y.; Zheng, G.; Noonan, A. F. *J. Org. Chem.* **2001**, *66*, 8677. (b) Li, G. Y. *Angew. Chem., Int. Ed.* **2001**, *40*, 1513. (c) Jiang, X.-b.; Minnaard, A. J.; Hessen, B.; Feringa, B. L.; Duchateau, A. L. L.; Andrien, J. G. O.; Boogers, J. A. F.; de Vries, J. G. *Org. Lett.* **2003**, *5*, 1503. (d) Jiang, X.-b.; van den Berg, M.; Minnaard, A. J.; Feringa, B. L.; de Vries, J. G. *Tetrahedron: Asymmetry* **2004**, *15*, 2223. (e) Bigeault, J.; Giordano, L.; Buono, G. *Angew. Chem., Int. Ed.* **2005**, *44*, 4753. (f) Ackermann, L. *Synthesis* **2006**, 1557. (g) Ackermann, L. *Synlett* **2007**, 507. (h) Ackermann, L. *Isr. J. Chem.* **2010**, *50*, 652. (i) Gatineau, D.; Moraleda, D.; Naubron, J.-V.; Bürgi, T.; Giordano, L.; Buono, G. *Tetrahedron: Asymmetry* **2009**, *20*, 1912. (j) Landert, H.; Spindler, F.; Wyss, A.; Blaser, H.-U.; Pugin, B.; Ribourduoille, Y.; Gschwend, B.; Ramalingam, B.; Pfaltz, A. *Angew. Chem., Int. Ed.* **2010**, *49*, 6873. (k) Achard, T.; Lepronier, A.; Gimbert, Y.; Clavier, H.; Giordano, L.; Tenaglia, A.; Buono, G. *Angew. Chem., Int. Ed.* **2011**, *50*, 3552. (l) Christiansen, A.; Selent, D.; Spannenberg, A.; Köckerling, M.; Reinke, H.; Baumann, W.; Jiao, H.; Franke, R.; Börner, A. *Chem.—Eur. J.* **2011**, *17*, 2120. (m) Kurscheid, B.; Belkoura, L.; Hoge, B. *Organometallics* **2012**, *31*, 1329. (n) Shaikh, T. M.; Weng, C.-M.; Hong, F.-E. *Coord. Chem. Rev.* **2012**, *256*, 771. (o) Dong, K.; Wang, Z.; Ding, K. *J. Am. Chem. Soc.* **2012**, *134*, 12474. (p) Schröder, F.; Tugny, C.; Salanouve, E.; Clavier, H.; Giordano, L.; Moraleda, D.; Gimbert, Y.; Mouriès-Mansuy, V.; Goddard, J.-P.; Fensterbank, L. *Organometallics* **2014**, *33*, 4051.

(13) Lu, J.; Aydin, C.; Browning, N. D.; Gates, B. C. *J. Am. Chem. Soc.* **2012**, *134*, 5022.

(14) Rafter, E.; Gutmann, T.; Löw, F.; Buntkowsky, G.; Philippot, K.; Chaudret, B.; van Leeuwen, P. W. N. M. *Catal. Sci. Technol.* **2013**, *3*, 595.

(15) Cano, I.; Chapman, A. M.; Urakawa, A.; van Leeuwen, P. W. N. M. *J. Am. Chem. Soc.* **2014**, *136*, 2520.

(16) (a) Lo, A. Y. H.; Sudarsan, V.; Sivakumar, S.; van Veggel, F.; Schurko, R. W. *J. Am. Chem. Soc.* **2007**, *129*, 4687. (b) Zhang, B.; Yan, B. *Anal. Bioanal. Chem.* **2010**, *396*, 973. (c) Gutmann, T.; del Rosal, I.; Chaudret, B.; Poteau, R.; Limbach, H.-H.; Buntkowsky, G. *ChemPhysChem* **2013**, *14*, 3026. (d) Gutmann, T.; Grünberg, A.; Rothermel, N.; Werner, M.; Srour, M.; Abdulhussain, S.; Tan, S.; Xu, Y.; Breitzke, H.; Buntkowsky, G. *Solid State Nucl. Magn. Reson.* **2013**, *55−56*, 1.

(17) (a) Sharma, R.; Holland, G. P.; Solomon, V. C.; Zimmermann, H.; Schiffenhaus, S.; Amin, S. A.; Buttry, D. A.; Yarger, J. L. *J. Phys. Chem. C* **2009**, *113*, 16387. (b) Sharma, R.; Taylor, R. E.; Bouchard, L.-S. *J. Phys. Chem. C* **2011**, *115*, 3297.

(18) Stefanescu, D.; Glueck, D.; Siegel, R.; Wasylishen, R. *J. Cluster Sci.* **2008**, *19*, 445.

(19) Song, S. G.; Satheeshkumar, C.; Park, J.; Ahn, J.; Premkumar, T.; Lee, Y.; Song, C. *Macromolecules* **2014**, *47*, 6566.

(20) (a) Dorris, A.; Rucareanu, S.; Reven, L.; Barrett, C. J.; Lennox, R. B. *Langmuir* **2008**, *24*, 2532. (b) Shaw, C. P.; Middleton, D. A.; Volk, M.; Lévy, R. *ACS Nano* **2012**, *6*, 1416.

(21) Guo, C.; Hall, G. N.; Addison, J. B.; Yarger, J. L. *RSC Adv.* **2015**, *5*, 1937.

(22) See the following for a variety of examples related to AuNPs of thiolates prepared with high selectivity: (a) Zhu, M.; Lanni, E.; Garg, N.; Bier, M. E.; Jin, R. *J. Am. Chem. Soc.* **2008**, *130*, 1138. (b) Zhu, M.; Aikens, C. M.; Hollander, F. J.; Schatz, G. C.; Jin, R. *J. Am. Chem. Soc.* **2008**, *130*, 5883. (c) Zhu, M.; Eckenhoff, W. T.; Pintauer, T.; Jin, R. *J. Phys. Chem. C* **2008**, *112*, 14221. (d) Wu, Z.; Suhan, J.; Jin, R. *J. Mater. Chem.* **2009**, *19*, 622. (e) Jin, R.; Eah, S.-K.; Pei, Y. *Nanoscale* **2012**, *4*, 4026. (f) Pei, Y.; Zeng, X. C. *Nanoscale* **2012**, *4*, 4054. (g) Kumar, S.; Jin, R. *Nanoscale* **2012**, *4*, 4222. (h) Dolamic, I.; Knoppe, S.; Dass, A.; Bürgi, T. *Nat. Commun.* **2012**, *3*, No. 798. (i) Li, G.; Jin, R. *Acc. Chem. Res.* **2013**, *46*, 1749 and references therein..

(23) See the following for a variety of examples related to thiolate−thiolate exchange for AuNPs: (a) Dass, A.; Holt, K.; Parker, J. F.; Feldberg, S. W.; Murray, R. W. *J. Phys. Chem. C* **2008**, *112*, 20276. (b) Si, S.; Gautier, C.; Boudon, J.; Taras, R.; Gladiali, S.; Bürgi, T. *J. Phys. Chem. C* **2009**, *113*, 12966. (c) Hadley, A.; Aikens, C. M. *J. Phys. Chem. C* **2010**, *114*, 18134. (d) Bresee, J.; Maier, K. E.; Melander, C.; Feldheim, D. L. *Chem. Commun.* **2010**, *46*, 7516. (e) Heinecke, C. L.; Ni, T. W.; Malola, S.; Mäkinen, V.; Wong, O. A.; Häkkinen, H.; Ackerson, C. J. *J. Am. Chem. Soc.* **2012**, *134*, 13316. (f) Knoppe, S.; Dass, A.; Burgi, T. *Nanoscale* **2012**, *4*, 4211. (g) Knoppe, S.; Bürgi, T. *Acc. Chem. Res.* **2014**, *47*, 1318 and references therein..

(24) AbdulHalim, L. G.; Kothalawala, N.; Sinatra, L.; Dass, A.; Bakr, O. M. *J. Am. Chem. Soc.* **2014**, *136*, 15865.

(25) Alternatively, a disproportionation may take place to small molecular compounds and clusters with high ligand content and gold metal.

(26) Link, S.; El-Sayed, M. A. *Annu. Rev. Phys. Chem.* **2003**, *54*, 331.

(27) Huertos, M. A.; Cano, I.; Bandeira, N. A. G.; Benet-Buchholz, J.; Bo, C.; van Leeuwen, P. W. N. M. *Chem.—Eur. J.* **2014**, *20*, 16121.

(28) We noted a systematic error between EA (in duplicate) and EDX (repeated up to 5 times), which are both reproducible within their standard errors. EDX always gives lower Au/P ratios than EA.

(29) Van Hardeveld, R.; Hartog, F. *Surf. Sci.* **1969**, *15*, 189.

(30) (a) Corthey, G.; Giovanetti, L. J.; Ramallo-López, J. M.; Zelaya, E.; Rubert, A. A.; Benitez, G. A.; Requejo, F. G.; Fonticelli, M. H.; Salvarezza, R. C. *ACS Nano* **2010**, *4*, 3413. (b) Behera, M.; Ram, S. *Appl. Nanosci.* **2014**, *4*, 247. (c) Battocchio, C.; Porcaro, F.; Mukherjee, S.; Magnano, E.; Nappini, S.; Fratoddi, I.; Quintiliani, M.; Russo, M. V.; Polzonetti, G. *J. Phys. Chem. C* **2014**, *118*, 8159. (d) Kiss, J.; Pusztai, P.; Ovari, L.; Baan, K.; Merza, G.; Erdoehelyi, A.; Kukovecz, A.; Konya, Z. *e-J. Surf. Sci. Nanotechnol.* **2014**, *12*, 252. (e) Park, J.-W.; Shumaker-Parry, J. S. *ACS Nano* **2015**, *9*, 1665.

(31) Odio, O. F.; Lartundo-Rojas, L.; Santiago-Jacinto, P.; Martínez, R.; Reguera, E. *J. Phys. Chem. C* **2014**, *118*, 2776.

(32) (a) Jean, G. E.; Michael, B. G. *Geochim. Cosmochim. Acta* **1985**, *49*, 979. (b) Mikhlin, Y. L.; Romanchenko, A. S.; Asanov, I. P. *Geochim. Cosmochim. Acta* **2006**, *70*, 4874.

(33) (a) Brust, M.; Walker, M.; Bethell, D.; Schiffrin, D. J.; Whyman, R. *J. Chem. Soc., Chem. Commun.* **1994**, *7*, 801. (b) Tang, Z.; Xu, B.; Wu, B.; Germann, M. W.; Wang, G. *J. Am. Chem. Soc.* **2010**, *132*, 3367.

(34) Ramirez, E.; Eradès, L.; Philippot, K.; Lecante, P.; Chaudret, B. *Adv. Funct. Mater.* **2007**, *17*, 2219.

(35) Bak, M.; Rasmussen, J. T.; Nielsen, N. C. *J. Magn. Reson.* **2000**, *147*, 296.

(36) Magiera, D.; Szmigielska, A.; Pietrusiewicz, K. M.; Duddeck, H. *Chirality* **2004**, *16*, 57.

(37) Power, W. P. *J. Am. Chem. Soc.* **1995**, *117*, 1800.

(38) (a) Mertens, P. G. N.; Poelman, H.; Ye, X.; Vankelecom, I. F. J.; Jacobs, P. A.; De Vos, D. E. *Catal. Today* **2007**, *122*, 352. (b) Mertens, P. G. N.; Vandezande, P.; Ye, X.; Poelman, H.; Vankelecom, I. F. J.; De Vos, D. E. *Appl. Catal., A* **2009**, *355*, 176. (c) Biondi, I.; Laurenczy, G. b.; Dyson, P. J. *Inorg. Chem.* **2011**, *50*, 8038.

(39) (a) Guzman, J.; Gates, B. C. *Angew. Chem., Int. Ed.* **2003**, *42*, 690. (b) Zanella, R.; Louis, C.; Giorgio, S.; Touroude, R. *J. Catal.* **2004**, *223*, 328.

(40) Herron, N.; Thorn, D. L. *Adv. Mater.* **1998**, *10*, 1173.

(41) (a) Zhu, H.; Ke, X.; Yang, X.; Sarina, S.; Liu, H. *Angew. Chem., Int. Ed.* **2010**, *49*, 9657. (b) Liu, X.; Ye, S.; Li, H.-Q.; Liu, Y.-M.; Cao, Y.; Fan, K.-N. *Catal. Sci. Technol.* **2013**, *3*, 3200. (c) Morales-Guio, C.; Yuranov, I.; Kiwi-Minsker, L. *Top. Catal.* **2014**, *57*, 1526.

(42) (a) Campos, C. H.; Jofré, M.; Torres, C. C.; Pawelec, B.; Fierro, J. L. G.; Reyes, P. *Appl. Catal. A: General* **2014**, *482*, 127 and references therein.. (b) Guan, Y.; Hensen, E. J. M. *Phys. Chem. Chem. Phys.* **2009**, *11*, 9578.

(43) Nigra, M. M.; Ha, J.-M.; Katz, A. *Catal. Sci. Technol.* **2013**, *3*, 2976 and references therein. This reference also reports a ligand effect: a phosphine enhances the reaction but certain thiols inhibit the reaction.

(44) Panayotov, D. A.; Burrows, S. P.; Yates, J. T.; Morris, J. R. *J. Phys. Chem. C* **2011**, *115*, 22400.

(45) Boronat, M.; Concepción, P.; Corma, A. *J. Phys. Chem. C* **2009**, *113*, 16772.

(46) Boronat, M.; Illas, F.; Corma, A. *J. Phys. Chem. A* **2009**, *113*, 3750.

(47) (a) Widegren, J. A.; Finke, R. G. *J. Mol. Catal. A-Chem.* **2003**, *198*, 317. (b) Finney, E. E.; Finke, R. G. *Inorg. Chim. Acta* **2006**, *359*, 2879. (c) Bayram, E.; Linehan, J. C.; Fulton, J. L.; Roberts, J. A. S.; Szymczak, N. K.; Smurthwaite, T. D.; Özkar, S.; Balasubramanian, M.; Finke, R. G. *J. Am. Chem. Soc.* **2011**, *133*, 18889. (d) Bayram, E.; Finke, R. G. *ACS Catal.* **2012**, *2*, 1967. (e) Sonnenberg, J. F.; Coombs, N.; Dube, P. A.; Morris, R. H. *J. Am. Chem. Soc.* **2012**, *134*, 5893.